Optimizing Parameters and Applications of Femtosecond Laser Technology in Fiber Bragg Grating Manufacture

Zhaoxu Han *

School of Electrical and Electronic Engineering, Nanyang Technological University, Singapore

* Corresponding Author Email: HANZ0019@e.ntu.edu.sg

Abstract. Fiber Bragg Grating (FBG) sensors have garnered extensive attention for their pivotal role in diverse domains, including strain, pressure, hydroacoustics, and temperature monitoring, especially within the ambit of the Internet of Things (IoT). The femtosecond laser point-by-point fabrication methodology stands out in this context, primarily for its flexibility in altering FBG periods through precise control of the fiber's movement velocity. This adaptability facilitates the creation of FBGs with varied periodicities, significantly broadening their application spectrum. A notable aspect of FBG sensors is their sensitivity to temperature variations, which manifest as changes in both the grating pitch and the refractive index of the FBG. These alterations consequently induce shifts in the FBG's reflection and transmission spectra. Specifically, temperature fluctuations lead to a discernible drift in the central wavelength of the light reflected by the Bragg grating. This wavelength drift is linearly proportional to the temperature change, rendering it a reliable metric for assessing both the magnitude and rate of temperature variations. Experimental framework was centered around the femtosecond laser point-by-point fabrication technique for FBG creation. Within this setup, we delved into four critical factors influencing the spectral quality of the FBGs: grating length, periodicity, laser energy, and grating position. By meticulously adjusting these parameters, we aimed to optimize the performance and applicability of FBG sensors in real-world IoT scenarios.

Keywords: Fiber Bragg Grating, femtosecond laser, fiber optic sensing.

1. Introduction

Femtosecond laser point-by-point inscription is a novel, fast, efficient, and flexible method for fabricating fiber Bragg gratings (FBGs). This method involves focusing a femtosecond laser into the core of an optical fiber and using programmed modulation to create refractive index changes within the fiber core to form the FBG. The technique utilizes three nonlinear effects of femtosecond lasers: multiphoton ionization, avalanche ionization, and tunnel ionization, to achieve micrometer-scale laser processing.

The interaction mechanism between femtosecond lasers and quartz material is primarily based on nonlinear effects. By adjusting the energy of the femtosecond laser, the laser beam's intensity in the focused central region can satisfy the conditions for multiphoton absorption in the quartz material, allowing the femtosecond laser to act within a very small area [1-4].

Femtosecond lasers are high-power ultrafast pulsed lasers that primarily operate through the thermal-optical effect. When they interact with a medium, the effective refractive index within the material can undergo periodic changes. Compared to other fabrication methods, FBGs fabricated using femtosecond lasers have the advantage of high-temperature stability. Over the past decade, the fabrication of FBGs using femtosecond lasers has received widespread attention and application [5, 6].

2. Femtosecond Laser Point-by-Point Writing System

Recent literature and experimental studies have established a correlation between the spectral quality of Fiber Bragg Gratings fabricated via femtosecond laser point-by-point writing and parameters such as grating period and length. The central wavelength of the laser in use is 1030 nm, which, upon passing through an integrated second harmonic generation module, yields an output wavelength of 515 nm [7]. This process employs an ASE (Amplified Spontaneous Emission) light

source. the selection of a broadband light source is contingent upon its spectral range. Available options include LED, ASE, and SLD (Superluminescent Diode) light sources. LED sources, characterized by a spectral range below 1000 nm, typically utilize multimode fibers, contrasting with the single-mode fibers employed in our experiment. SLD sources, operating on the principle of super-radiant emission from semiconductor devices, generate a broad spectrum, typically around 800 nm, 1300 nm, and 1550 nm [8]. Their broad spectrum arises from the distribution of electrons and holes across multiple energy levels. In contrast, ASE light sources amplify spontaneous emission through gain media [9]. Both SLD and ASE sources, prevalent in optical measurement and sensing systems, offer broad spectral ranges and low coherence. The choice between them hinges on application-specific requirements: SLDs for a wider spectral range and ASEs for better spectral flatness [10]. In our experiment, we utilize an ASE source with a central wavelength of 515 nm. Laser intensity is meticulously controlled using attenuators with specific attenuation ratios (e.g., external attenuator at 50% and internal attenuator at 30%), aiming for an optimal intensity of 114 nJ. The light of a specific wavelength is then reflected using a dichroic mirror, which, unlike a half-mirror lens, selects light based on wavelength. The use of a dichroic mirror results in particularly bright light spots on the computer screen when observed with a CCD camera, whereas a half-mirror lens yields unsuitable green light spots [11]. Employing an oil-immersion objective lens enhances the circularity of the fabricated FBG. The displacement platform comprises Aerotech ABL1000WB, ABL1000, and ANT130V-5 air-bearing electric stages, complemented by a rotating fixture holder for sample manipulation [12]. The refractive index modulation in the treated area is intrinsically linked to the laser energy post-external optical path traversal. At lower energy levels, the refractive index and density in the modulated region increase, yielding isotropic modulation. Conversely, at higher energies, plasma explosions may damage the quartz structure, creating cracks or microcavities. Lastly, a high-quality imaging observation system is pivotal for precise localization and assessment of the light. As shown in Fig 1.

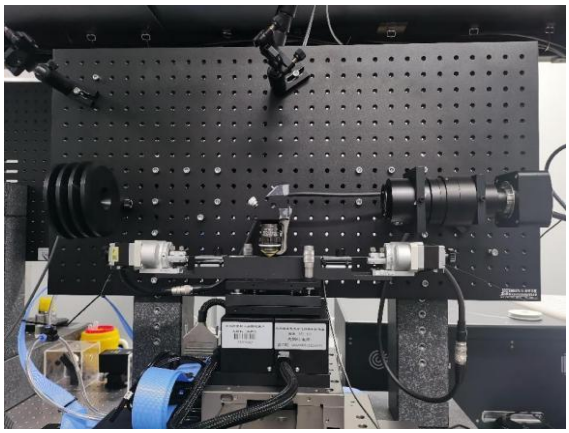

Figure 1. Photograph of the setup for femtosecond laser point-by-point fabrication of FBGs (Photo/Picture credit: Original).

3. Parameters Impacting the Fabrication of Fiber Bragg Gratings (FBGs) Using Femtosecond Laser

The process of fabricating Fiber Bragg Gratings via femtosecond laser systems encompasses several meticulous steps: Preparation of Optical Fiber: Initially, the optical fiber's coating layer is removed from a designated section, followed by a thorough cleaning with alcohol. The fiber is then positioned on a sample holder, securely clamped, and aligned on a three-dimensional motorized stage [13]. Glycerin Application for Enhanced Imaging: A droplet of glycerin is placed on a glass slide, and the microscope's objective lens is gently touched against the glycerin-coated side. This step ensures a thin glycerin film on the lens, facilitating clearer visualization of the fiber core. Laser Beam Alignment: The femtosecond laser beam is aligned to enter the center of the fiber core perpendicularly

through the objective lens. The motorized stage's x-axis movement is synchronized with the laser beam, allowing for consistent observation of the fabricated FBG from multiple angles [14]. FBG Fabrication Programming: Utilizing the system's software, the FBG is fabricated point-by-point. Critical parameters such as the motorized stage's x-axis speed, grating period, and length are meticulously set to achieve the desired FBG functionality. Laser Power Adjustment: The power of the femtosecond laser is finely tuned using either an internal or external energy attenuator, according to the requirements of the FBG. Fabrication and Inspection: The programmed fabrication process is executed. Post-fabrication, the FBG undergoes a thorough inspection to ensure it meets the set specifications and exhibits no displacement [15]. Adjustments in the program's parameters and the laser's energy level enable the fabrication of FBGs with diverse specifications.

Two primary challenges may arise during FBG fabrication: Alignment Inconsistency: In cases where the FBG's axis does not maintain a horizontal alignment, likely due to imprecise leveling of the sample holder, the knobs on the holder are utilized for fine adjustments. This ensures the FBG's central positioning within the fiber core, aligning its axis horizontally [16]. FBG Length Control: The absence of an electric shutter on the control panel can lead to difficulties in controlling the FBG length accurately. To mitigate this, FBGs are fabricated multiple times, enhancing the precision of the resultant lengths.

3.1. Influence of Grating Length on Fiber Bragg Gratings

To elucidate the impact of varying grating lengths on the transmission and reflection spectra of Fiber Bragg Gratings, a controlled experimental setup was established. Parameters included a single pulse laser energy of 114 nJ, a pulse frequency (f) of 0.1 kHz, and a precision three-dimensional displacement platform operating at an x-axis speed (v) of 0.1071 mm/s. In the transmission spectrum, distinct trends were observed with increasing FBG lengths. For a 1 mm FBG (deep blue fine line), the transmission peak depth was noted at 5 dB, with a reflectivity of 68.4% and a central wavelength of 1548.92 nm. Progressively, for the 2 mm FBG (red fine line), the peak depth increased to 12 dB, reflectivity to 93.6%, and the central wavelength shifted to 1548.85 nm. This pattern continued with the 3 mm FBG (yellow fine line) showing a peak depth of 15 dB, reflectivity of 96.7%, and a central wavelength of 1548.94 nm. For the 4 mm (purple fine line) and 5 mm (green fine line) FBGs, peak depths reached 20 dB and 22 dB, reflectivities to 99.0% and 99.4%, and central wavelengths shifted to 1548.86 nm and 1548.8 nm, respectively. Finally, the 6 mm FBG (light blue fine line) exhibited a peak depth of 26 dB, reflectivity of 99.6%, and a central wavelength of 1549.21 nm. A maximum reflectivity of 99.7% was observed, indicating a narrowing bandwidth and deepening transmission peak with increased FBG length. In the reflection spectra, all FBG lengths (1 mm to 6 mm) demonstrated a consistent reflection peak intensity of 43 dB, though the central wavelengths varied minimally, in line with their transmission counterparts. This phenomenon aligns with existing literature, where FBG length does not significantly alter reflection peak intensity. Notably, Fig 2 reveals variations in the reflection peak bandwidth across different FBGs, potentially attributable to varied stress levels on the fibers during experimentation. Given laboratory constraints, fabricating a 6 mm FBG poses challenges. Consequently, our primary research focus will be on the 5 mm FBG, offering a balanced insight into the spectral characteristics pertinent to these lengths. As shown in Fig 3.

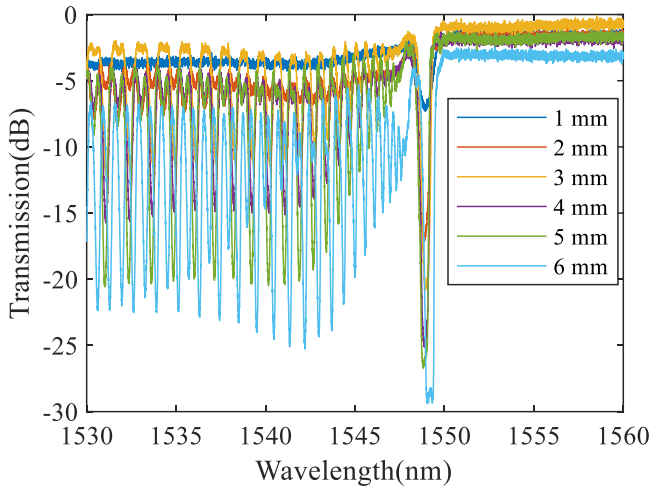

Figure 2. The transmission spectra of the FBGs with grating lengths of 1 mm, 2 mm, 3 mm, 4 mm, 5 mm, and 6 mm (Photo/Picture credit: Original).

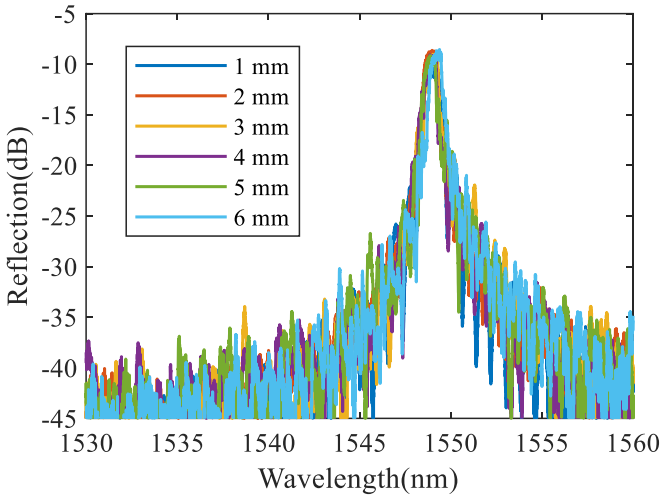

Figure 3. The reflection spectra of the FBGs with grating lengths of 1 mm, 2 mm, 3 mm, 4 mm, 5 mm, and 6 mm in (Photo/Picture credit: Original).

3.2. Impact of Grating Period on Fiber Bragg Gratings

The following parameters were set: grating length l = 5 mm, single pulse laser energy 114 nJ, laser pulse frequency f = 0.1 kHz. A three-dimensional displacement platform was used with x-axis movement speeds of 0.1065 mm/s, 0.1068 mm/s, 0.1071 mm/s, and 0.1074 mm/s. In all cases, the transmission peak depth is 22 dB, reflectivity is 99.4%, but the center wavelengths vary. All of them have a reflection peak intensity of 43 dB, but the center wavelengths vary.

Analysis of the reflection spectra of the four different period fiber Bragg gratings reveals that although the grating periods are different, the reflection intensities are consistent at 43 dB. The discrepancy in transmission spectra depth for some periods may be due to variations in stress on the fiber when placed in the fiber fixture during fabrication. The drift in center wavelength could be caused by differential stress during the manufacturing process or external factors such as bending or other applied stresses during measurement. As shown in Fig 4 and Fig 5.

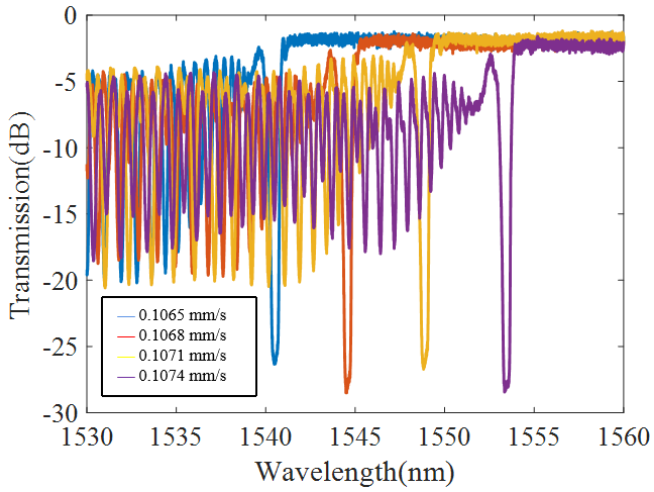

Figure 4. The transmission spectra of FBG1, FBG2, FBG3, and FBG4 (Photo/Picture credit: Original).

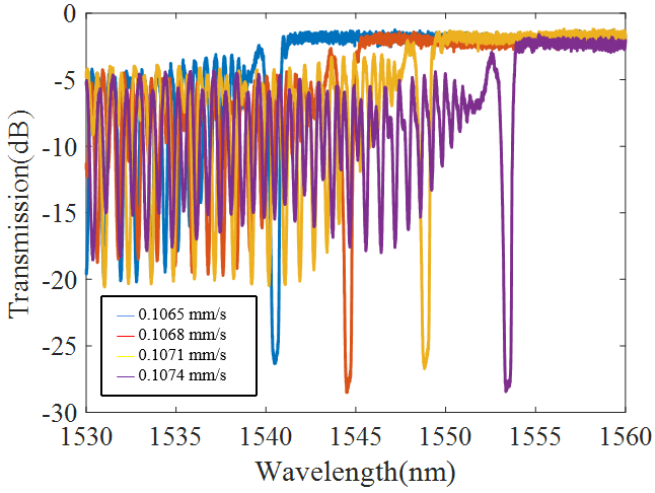

Figure 5. Displays the reflection spectra of FBG1, FBG2, FBG3, and FBG4 (Photo/Picture credit: Original).

3.3. Effect of Laser Energy on Fiber Bragg Gratings

In the conducted experiments, the following parameters were meticulously set: the grating length (l) was established at 5 mm, the laser pulse frequency (f) at 0.1 kHz, and the three-dimensional displacement platform was calibrated for an x-axis movement speed (v) of 0.1071 mm/s. We utilized single pulse laser energies of 125 nJ and 135 nJ. The resultant transmission and reflection spectra of the fabricated fiber Bragg grating (FBG) are delineated in Figures 4 and 5, respectively. Notably, the transmission spectrum of the FBG fabricated with a laser energy of 135 nJ is depicted by the red line. This spectrum is characterized by an enhanced peak depth of 27 dB and a reflectivity of 99.8%, with a central wavelength situated at 1549.23 nm. These results elucidate that an increment in laser energy correlates with a profounder transmission peak and augmented reflectivity in the fabricated FBG. Extensive review of relevant literature reveals that at relatively elevated laser energies, multiple sets of grating profiles, bearing identical periodicities and aligned parallelly, emerge within the fiber. An excessive laser energy amplifies the self-focusing effect and poses a risk of damaging the immersion objective lens. Conversely, at lower laser energies, the FBG's transmission peak depth and reflectivity are observed to diminish. Additionally, insufficient laser energy may result in blurred imagery when visualizing the FBG through a CCD on a computer screen. To circumvent these issues and mitigate the self-focusing effect—while safeguarding the objective lens against damage from excessive laser

energy—we employed a white light laser at an energy of 114 nJ. This approach not only prevented lens damage but also ensured the FBG's clear visibility on the computer screen, as demonstrated in Figures 6 and 7.

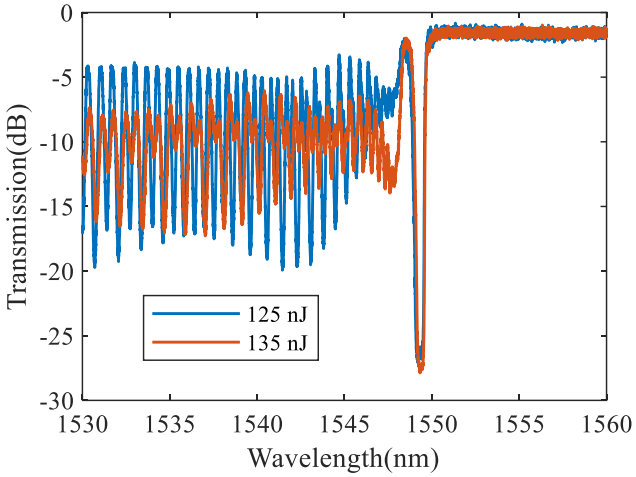

Figure 6. Shows the transmission spectra of FBGs fabricated with laser energies of 125 nJ and 135 nJ (Photo/Picture credit: Original).

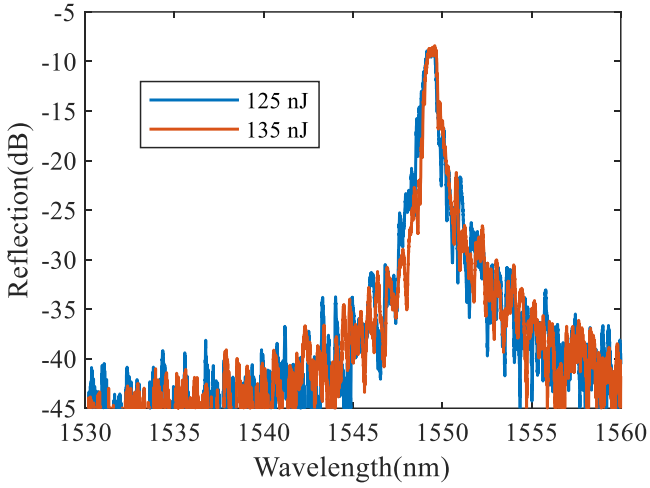

Figure 7. The reflection spectra of FBGs fabricated with laser energies of 125 nJ and 135 nJ (Photo/Picture credit: Original).

3.4. Role of Grating Position in Fiber Bragg Gratings

To study the relationship between grating position and the signal-to-noise ratio of FBG reflection peaks, the following parameters were set: grating length l=5 mm, laser pulse frequency f=0.1 kHz, three-dimensional displacement platform with x-axis movement speed v=0.1071 mm/s. Single pulse laser energy was set to 114 nJ. As shown in Fig 8.

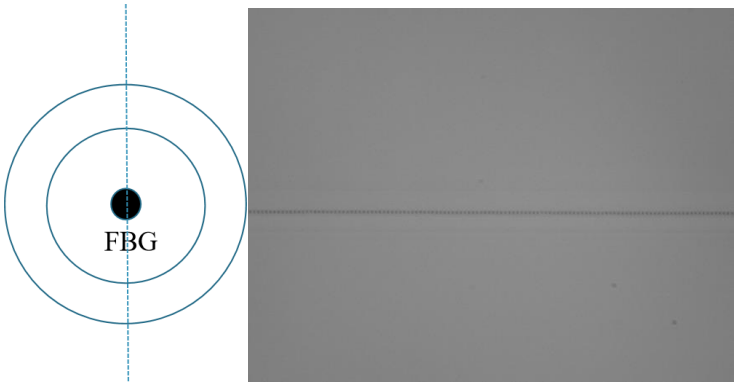

Figure 8. Side and Top Views of Fiber Bragg Grating Precisely Positioned at the Center of the Fiber Core (Photo/Picture Credit: Original).

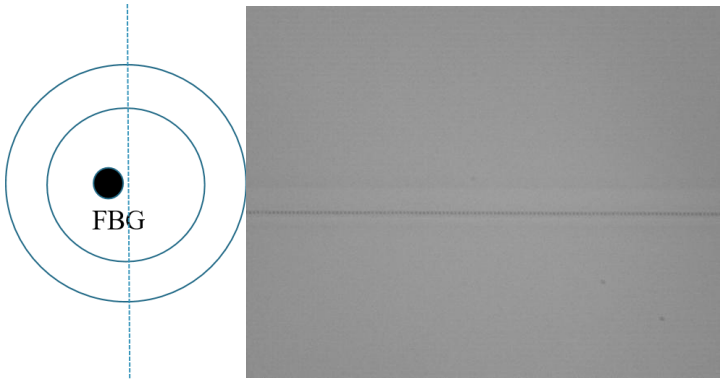

Figure 9. Side view Figure Top view Figure Fiber Bragg grating positioned at 1/4 distance from the fiber core (Photo/Picture credit: Original).

As shown in Fig 9-12. In the reflection spectrum, the blue line represents the reflection spectrum when the fiber Bragg grating is positioned at the center of the fiber core, with a reflection peak intensity of 43 dB and a central wavelength of 1549.32 nm. The yellow line represents the reflection spectrum when the fiber Bragg grating is positioned at the edge of the fiber core, with unchanged reflection peak intensity of 43 dB and an unchanged central wavelength of 1549.11 nm.

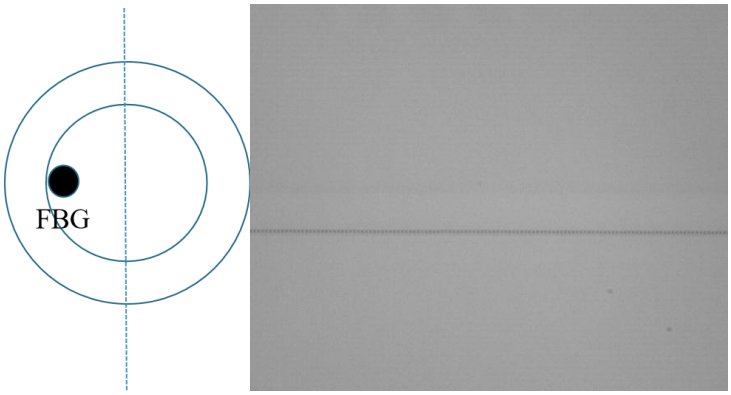

Figure 10. Side view Figure Top view Figure Fiber grating positioned at the edge of the core (Photo/Picture credit: Original).

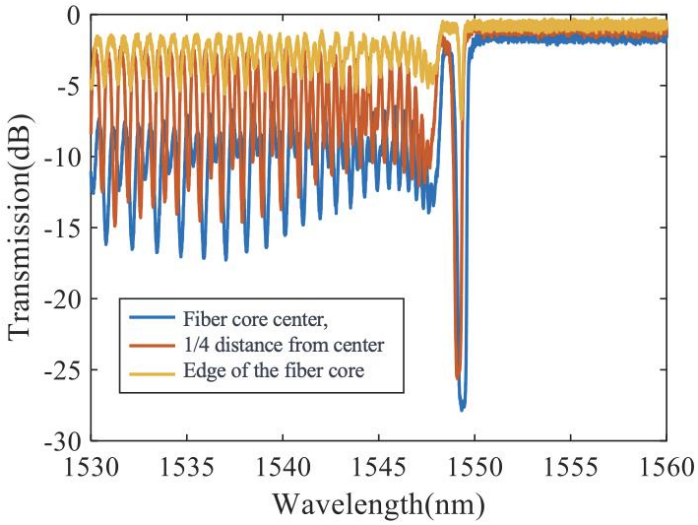

Figure 11. Transmission spectra of FBGs positioned at the center, 1/4 distance from the center, and the edge of the fiber core (Photo/Picture credit: Original).

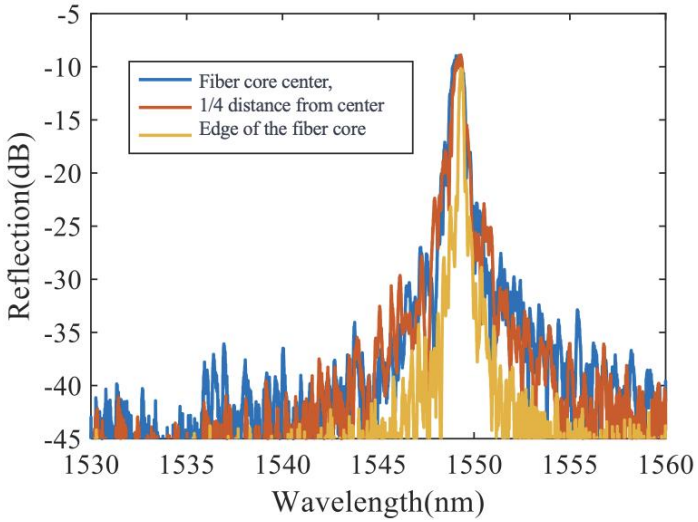

Figure 12. Reflection spectra of FBGs positioned at the center, 1/4 distance from the center, and the edge of the fiber core (Photo/Picture credit: Original).

From the transmission spectra, it can be observed that the reflectance of fiber Bragg gratings is dependent on their position within the fiber core. According to the theory of mode coupling in gratings, which is supported by relevant literature, light propagating through the fiber can be classified into low-order modes at the center and high-order modes at the edge. When the modulation region is located at the center, there is a larger overlap between the low-order mode and the modulation region, resulting in higher reflectance. The reflection wavelength of the low-order mode is in the longer wavelength range.

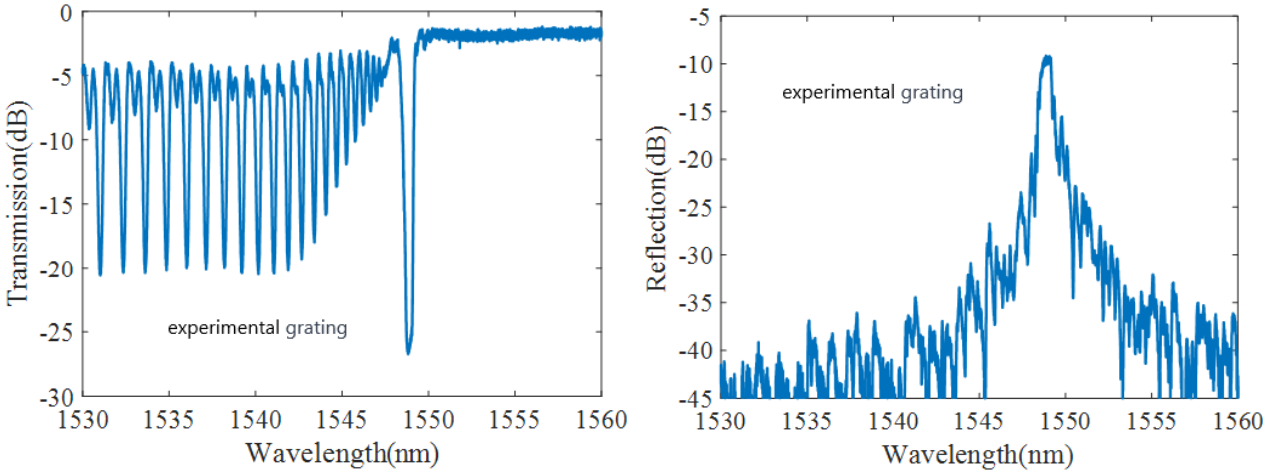

Figure 13. Spectra of FBGs fabricated using the femtosecond laser point-by-point method (Photo/Picture credit: Original).

4. Conclusion

Through meticulous comparative analysis, we have ascertained that the ideal laser energy for Fiber Bragg Grating (FBG) fabrication is 114 nJ. It is noteworthy that an increase in grating length correlates with enhanced reflectance in FBGs. However, this is juxtaposed with an increased complexity in the fabrication process. A pivotal aspect of our investigation was assessing the influence of the FBG's positional variance within the standard fiber on its transmission and reflection spectra. Our findings indicate that FBGs centrally located within the fiber manifest the most optimal optical properties, characterized by a transmission peak depth of 22 dB and an impressive reflectance of 99.4%. Conversely, when the FBG is positioned at a quarter length from the fiber core's center, there is a noticeable diminution in optical performance, evidenced by a reduction in the transmission peak depth to 20 dB and reflectance to 99.0%. The impact is more pronounced when the FBG is situated at the edge of the fiber core, where the transmission peak depth plummets to a mere 5 dB, and the reflectance sharply falls to 56.4%. As shown in Fig 13. Consequently, the FBG fabrication parameters are meticulously chosen as follows: a laser energy setting of 114 nJ, a grating length of 5 mm, and the positioning of the FBG at the central axis of the fiber core. These parameters are selected to optimize the reflectance and transmission characteristics of the FBGs, catering to the specific requirements of advanced optical sensing applications.

References

[1] J. Williams Robert, V. Christian, D. Marshall Graham, T. Andreas, N. Stefan, J. Steel M, J. Withford Michael. Point-by-point inscription of apodized fiber Bragg gratings [J]. Optics letters, 2011, 36 (15).

[2] M. Lenzner., S. Sartania, Z. Cheng, C. Spielmann, G. Mourou. W. Kautek, F. Krausz, J. Kruger. Femtosecond optical breakdown in dielectrics [J]. Physical review letters, 1998, 80 (18).

[3] S. Yang, D. Hu, A. Wang. Point-by-point fabrication and characterization of sapphire fiber Bragg gratings [J]. Optics letters, 2017, 42 (20).

[4] V. Dostovalov A, A. Wolf A, V. Parygin A, E. Zyubin V, A. Babin S. Femtosecond point-by-point inscription of Bragg gratings by drawing a coated fiber through ferrule [J]. Optics express, 2016, 24 (15).

[5] J. Mihailov Stephen, W. Smelser Christopher, P. Lu, B. Walker Robert, G. Dan, H. Ding, H. George, U. James. Fiber bragg gratings made with a phase mask and 800-nm femtosecond radiation [J]. Optics letters, 2003, 28 (12).

[6] A. Martinez, I. Y. Khrushchev, I. Bennion. Thermal properties of fibre Bragg gratings inscribed point-by-point by infrared femtosecond laser [J]. Electronics Letters, 2005, 41 (4).

[7] Wolf, A., Dostovalov, A., Bronnikov, K., Skvortsov, M., Wabnitz, S., & Babin, S. (2022). Advances in femtosecond laser direct writing of fiber Bragg gratings in multicore fibers: technology, sensor and laser applications. Opto-Electronic Advances, 5 (4), 210055.

[8] Xu, X., He, J., He, J., Xu, B., Chen, R., Yang, K., ... & Wang, Y. (2021). Slit beam sha** for femtosecond laser point-by-point inscription of high-quality fiber Bragg gratings. Journal of Lightwave Technology, 39 (15), 5142 - 5148.

[9] Chen, R., He, J., Xu, X., Wu, J., Wang, Y., & Wang, Y. (2022). High-Quality Fiber Bragg Gratings Inscribed by Femtosecond Laser Point-by-Point Technology. Micromachines, 13 (11), 1808.

[10] Viveiros, D., Amorim, V. A., Maia, J. M., Silva, S., Frazão, O., Jorge, P. A., ... & Marques, P. V. (2020). Femtosecond laser direct written off-axis fiber Bragg gratings for sensing applications. Optics & Laser Technology, 128, 106227.

[11] Zhu, X., Xu, H., Zhao, Z., & others. (2021). An Environmental Intrusion Detection Technology Based on WiFi. Wireless Personal Communications, 119 (2), 1425 - 1436.

[12] Zhang, J., Zhou, Y., Sun, P., Du, D., Cui, J., & Zhao, Q. (2023). Investigating key factors for optimizing FBG inscribed by femtosecond laser. Optics Communications, 528, 129049.

[13] Mihailov, S. J., Hnatovsky, C., Abdukerim, N., Walker, R. B., Lu, P., Xu, Y., ... & Grobnic, D. (2021). Ultrafast laser processing of optical fibers for sensing applications. Sensors, 21 (4), 1447.

[14] Han, Y., Guo, Y., Gao, B., Ma, C., Zhang, R., & Zhang, H. (2020). Generation, optimization, and application of ultrashort femtosecond pulse in mode-locked fiber lasers. Progress in Quantum Electronics, 71, 100264.

[15] He, J., He, J., Xu, X., Du, B., Xu, B., Liao, C., ... & Wang, Y. (2021). Single-mode helical Bragg grating waveguide created in a multimode coreless fiber by femtosecond laser direct writing. Photonics Research, 9 (10), 2052 - 2059.

[16] Sun, X., Chang, Z., Zeng, L., Dong, X., & Hu, Y. (2021). Wavelength tunable fiber Bragg gratings fabricated by stress annealing assisted femtosecond laser direct writing. Optical Fiber Technology, 61, 102427.